Electronic Supplementary Material (ESI) for Environmental Science: Nano.
This journal is © The Royal Society of Chemistry 2021

Supporting Information

Converting mesoporous polydopamine coated MIL-125 (Ti) to core-shell heterostructure for efficient water desalination

Hao Zhang, Chaohai Wang, Xiaodie Li, Jia Xie, Xin Yan, Junwen Qi, Xiuyun Sun, and Jiansheng Li*

Key Laboratory of Jiangsu Province for Chemical Pollution Control and Resources Reuse, School of Environmental and Biological Engineering, Nanjing University of Science and Technology, Nanjing 210094, China.

E-mail: lijsh@njust.edu.cn

Chemicals. Tetra-n-butyl titanate $Ti(OC_4H_9)_4$ was purchased from Sinopharm Chemical Reagent Co., Ltd. Terephthalic acid (H_2BDC), dopamine hydrochloride, and 1, 3, 5-trimethylbenzene (TMB) were purchased from Aladdin Industrial Corporation. Pluronic F127 and were purchased from Sigma-Aldrich. Carbon black was purchased from Alfa Aesar. Tris-buffer was purchased from Bio-Rad Laboratories, Inc. Polytetrafluoroethylene (PTFE), anhydrous ethanol, methanol, sodium chloride (NaCl), and N, N-dimethylformamide (DMF) were obtained from Nanjing Chemical Reagent Co., Ltd. All chemicals were used as received without further purification.

Materials Characterization. The morphology and structure of the samples were conducted by scanning electron microscopy (SEM, JEOL 7800 system) and transmission electron microscopy (TEM, FEI Tecnai G2 F30 S-Twin). The composition was investigated by X-ray diffraction (XRD, BRUKER D8, Cu Kα) at 40 kV and 40 mA (λ = 1.5418 Å). The N_2 adsorption-desorption isotherms were collected using the Micromeritics ASAP-2020 instrument. X-ray photoelectron spectroscopy (XPS) spectra were obtained by PHI Quantera II ESCA System with Al Kα radiation at 1486.8 V. Thermogravimetric analysis (TGA) measurements were conducted by the SDT Q600 thermogravimetry/differential thermal analyzer. Raman spectroscopy was conducted using the Renishaw in Via reflex spectrometer system. Fourier transform infrared (FTIR) spectra of the samples were obtained using FT-IR spectrometer (Bruker HYPERION, Germany).

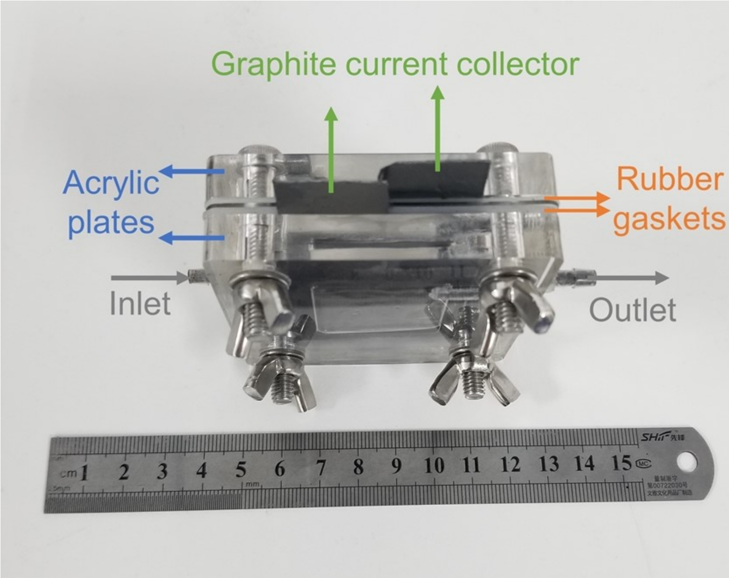

Fig. S1. The digital photograph of HCDI device.

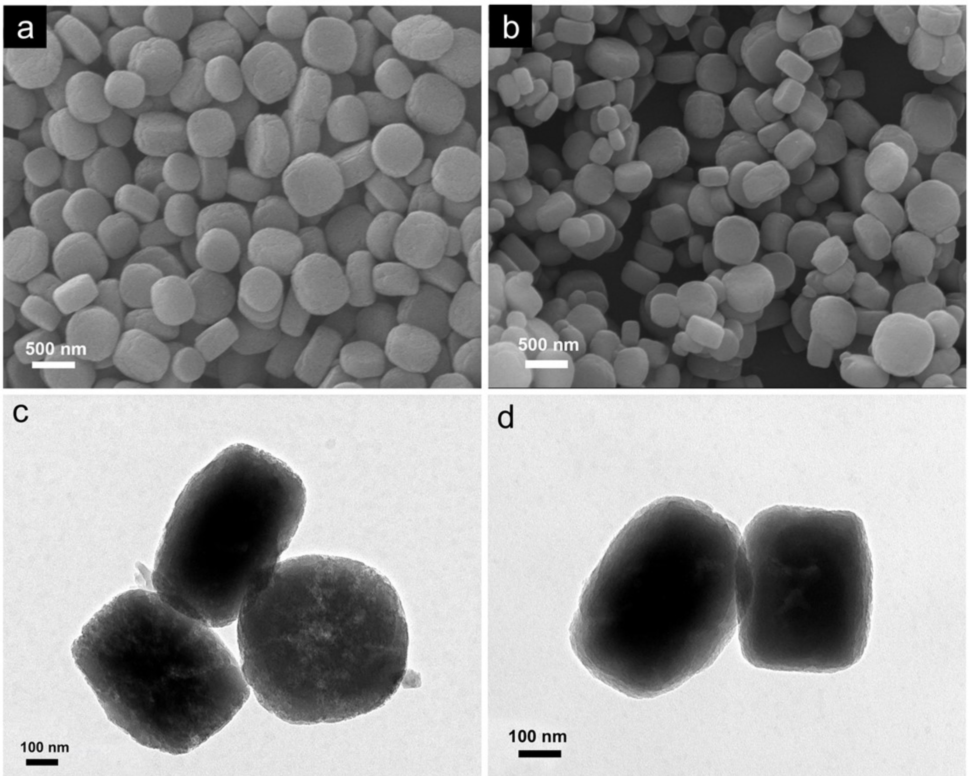

Fig. S2. (a) SEM image and (c) TEM image of MIL-125. (b) SEM image and (d) TEM image of MIL-125@PDA.

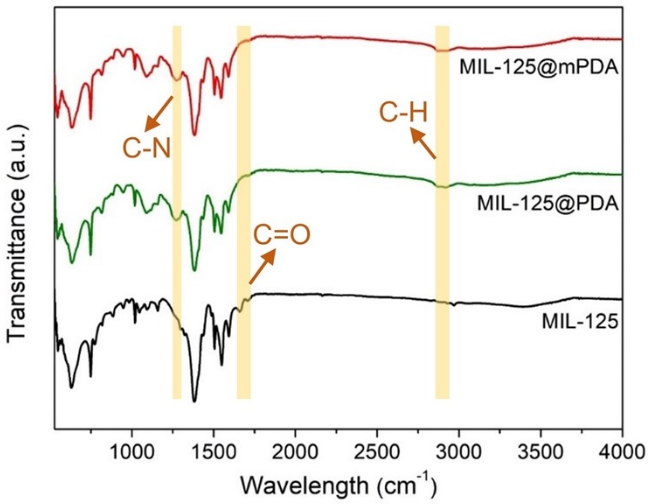

Fig. S3. Fourier transform infrared (FTIR) spectra of MIL-125, MIL-125@PDA, and MIL-125@mPDA.

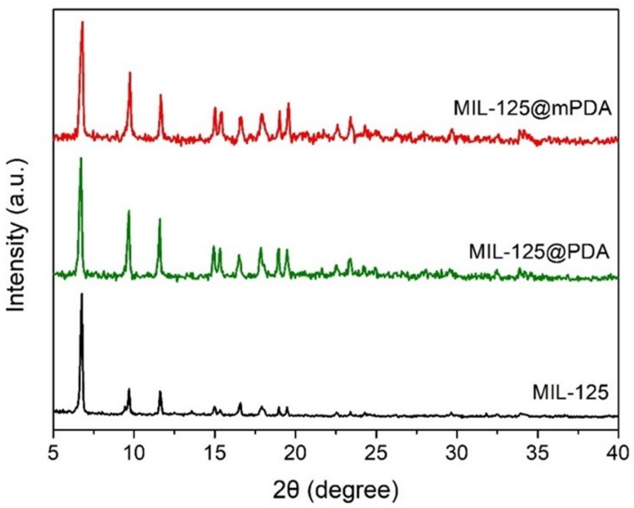

Fig. S4. X-ray diffraction (XRD) patterns of MIL-125, MIL-125@PDA, and MIL-125@mPDA.

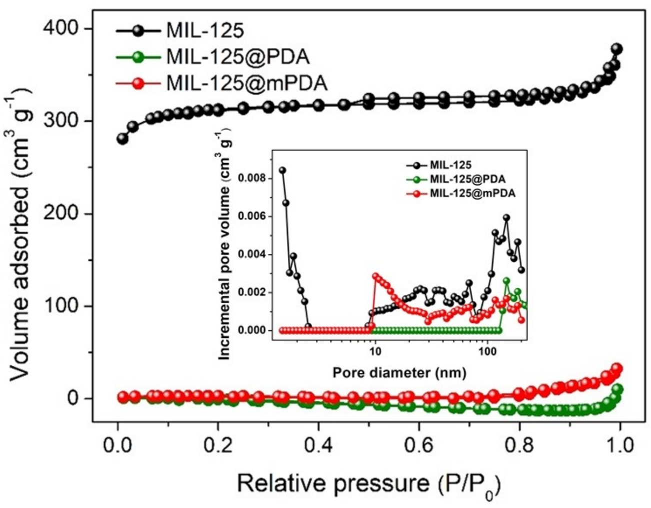

Fig. S5. N_2 adsorption/desorption isotherms and pore size distributions (insert) of MIL-125, MIL-125@PDA, and MIL-125@mPDA.

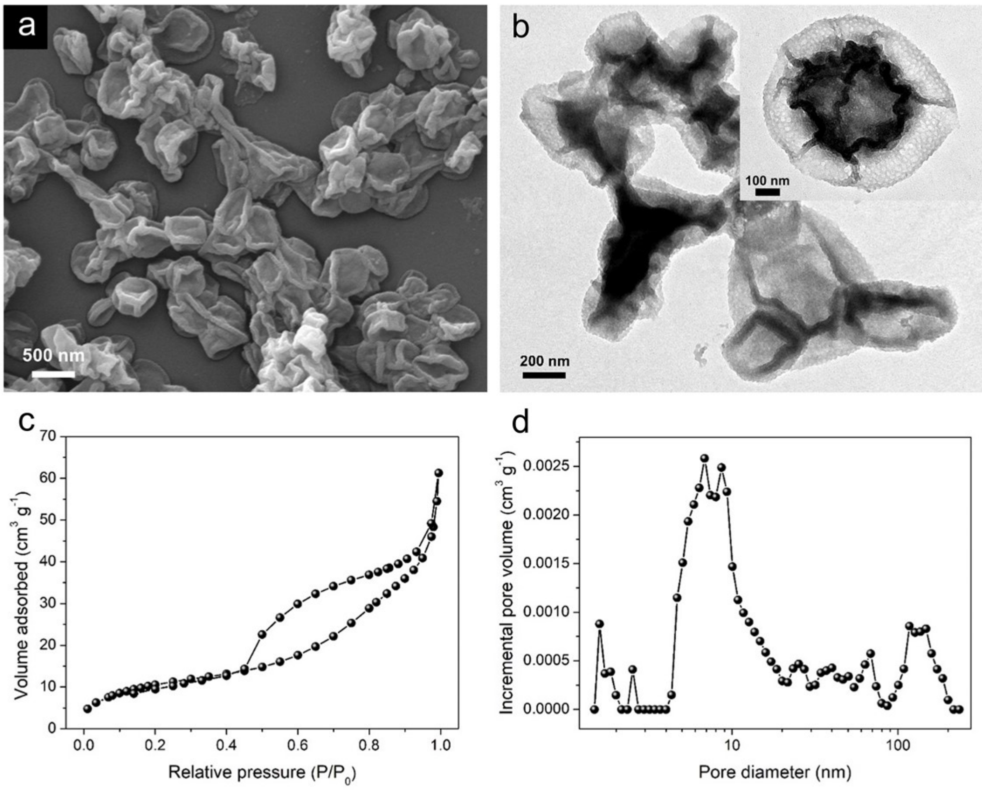

Fig. S6. (a) SEM image, (b) TEM image, (c) N_2 adsorption/desorption isotherm, and (d) pore size distribution of the mesostructured PDA shell after the alkali etching of MIL-125 core.

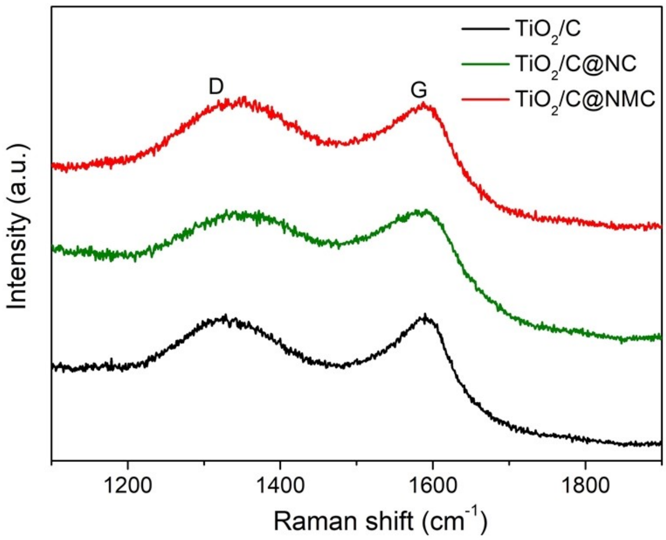

Fig. S7. Raman spectra ranging from 1100 cm^{-1} and 1900 cm^{-1} of TiO_2/C, TiO_2/C@NC, and TiO_2/C@NMC.

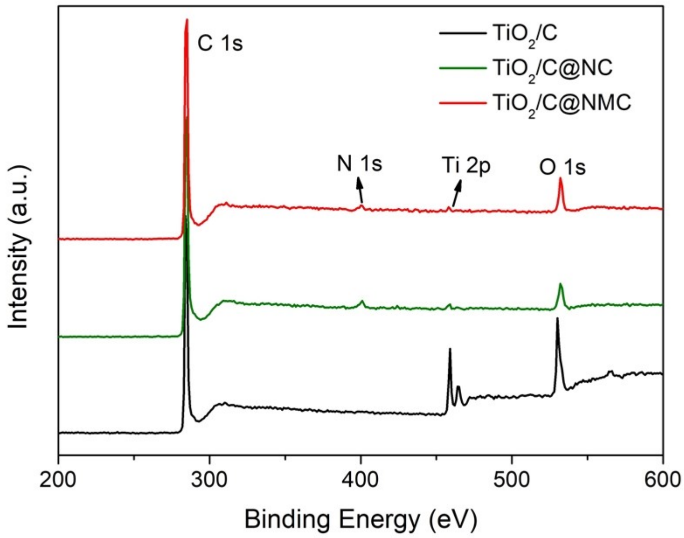

Fig. S8. XPS full surveys of TiO_2/C, TiO_2/C@NC, and TiO_2/C@NMC.

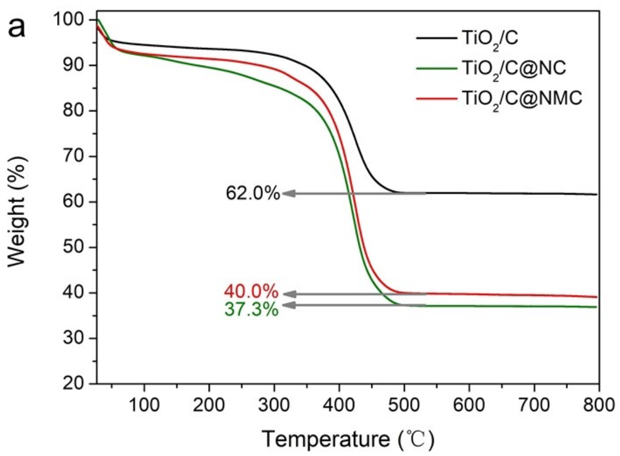

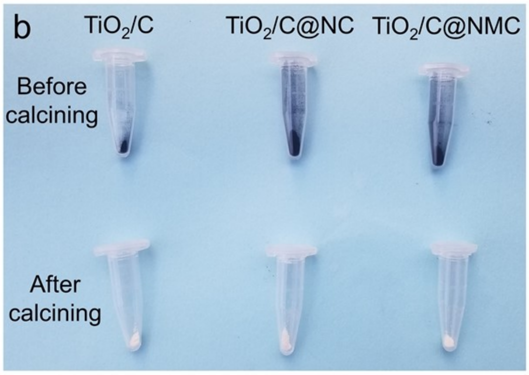

Fig. S9. (a) TGA curves of TiO_2/C, TiO_2/C@NC, and TiO_2/C@NMC tested in air atmosphere with a heating rate of 10 ^{o}C min^{-1} and (b) the digital photograph of TiO_2/C, TiO_2/C@NC, and TiO_2/C@NMC before and after calcining.

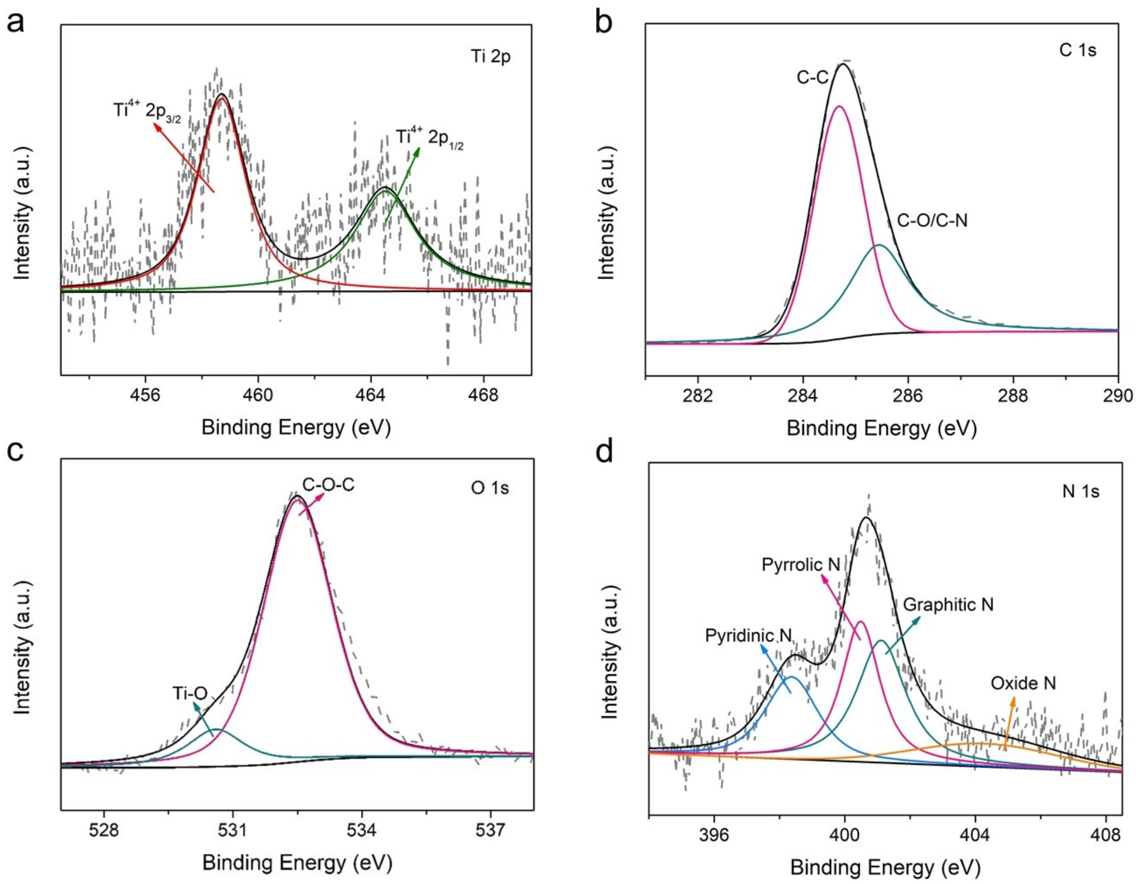

Fig. S10. (a) Ti 2p spectra, (b) C 1s spectra, (c) O 1s, and (d) N 1s of TiO_2/C@NMC.

Table S1. Structural parameters and elemental compositions of TiO_2/C, TiO_2/C@NC, and TiO_2/C@NMC.

Sample	S_{BET} ($m^2\ g^{-1}$)	V_{pore} ($cm^3\ g^{-1}$)	Surface elemental composition (%)				Ti content calculated by TGA (%)
			C	O	Ti	N	
TiO_2/C	330.6	0.22	79.9	14.6	5.5	/	37.1
TiO_2/C@NC	189.7	0.09	89.4	6.3	0.8	3.5	22.3
TiO_2/C@NMC	202.3	0.12	89.7	7.3	0.7	2.3	24.0

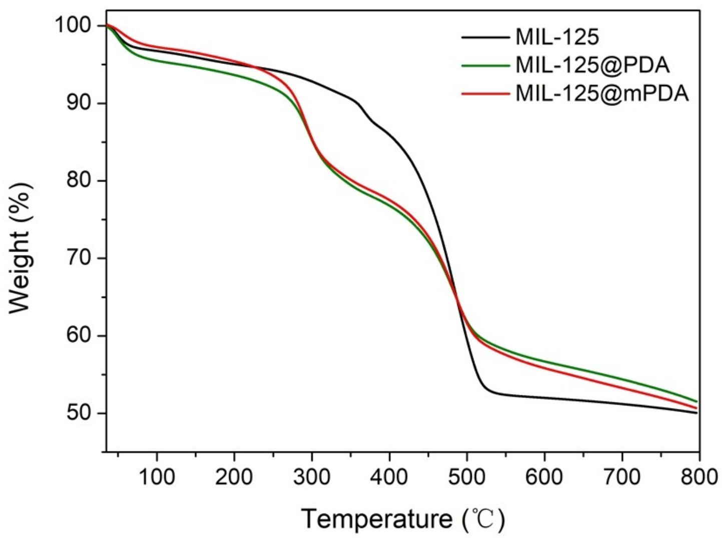

Fig. S11. TGA curves of MIL-125, MIL-125@PDA, and MIL-125@mPDA tested in N_2 atmosphere with a heating rate of 5 ^{o}C min^{-1}.

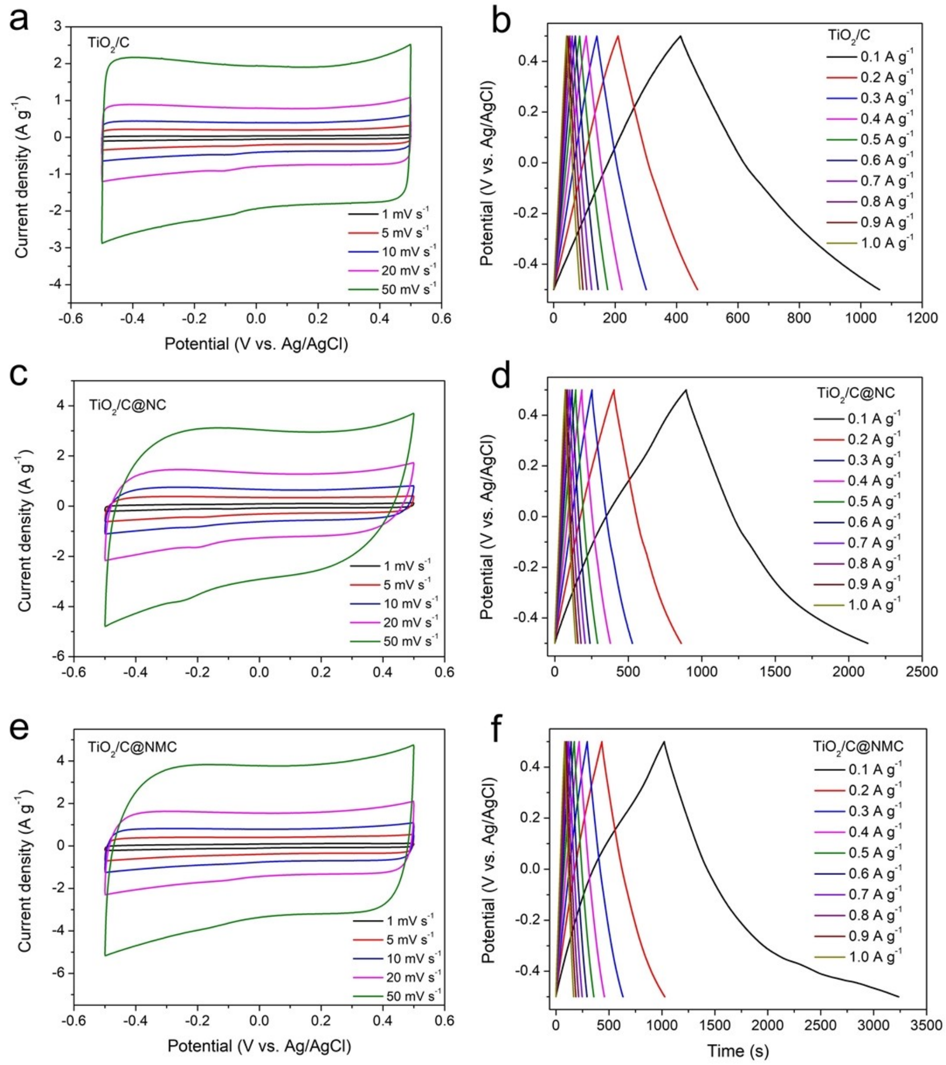

Fig. S12. CV curves and GCD plots of (a, b) TiO_2/C, (c, d) TiO_2/C@NC, and (e, f) TiO_2/C@NMC at different scan rates and current densities in 1 M NaCl solution.

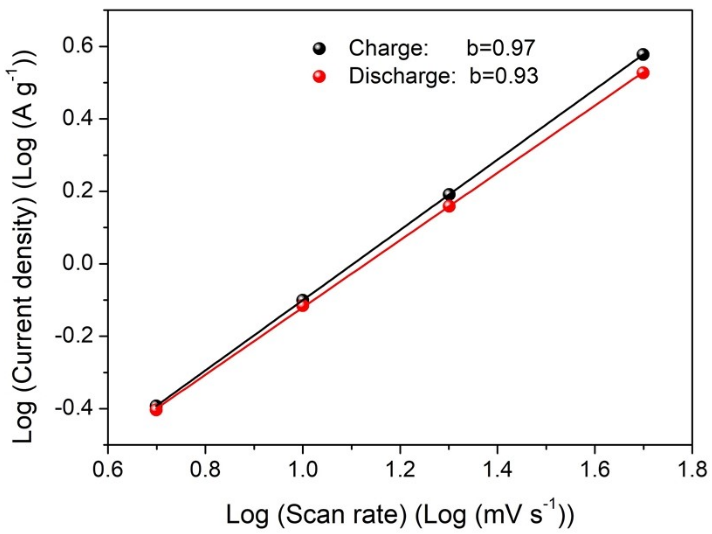

Fig. S13. The *b* values determined by using the relationship between the current density and the scan rate.

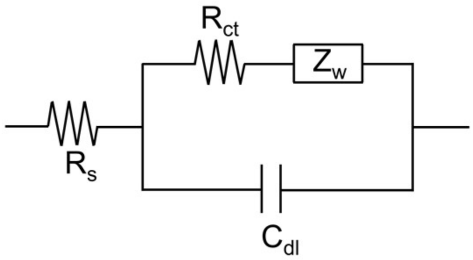

Fig. S14. The equivalent circuit diagram of EIS.

Table S2. R_s and R_{ct} of TiO_2/C, TiO_2/C@NC, and TiO_2/C@NMC electrodes.

Sample	R_s (Ω)	R_{ct} (Ω)
TiO_2/C	2.81	3.56
TiO_2/C@NC	2.84	3.33
TiO_2/C@NMC	2.71	2.72

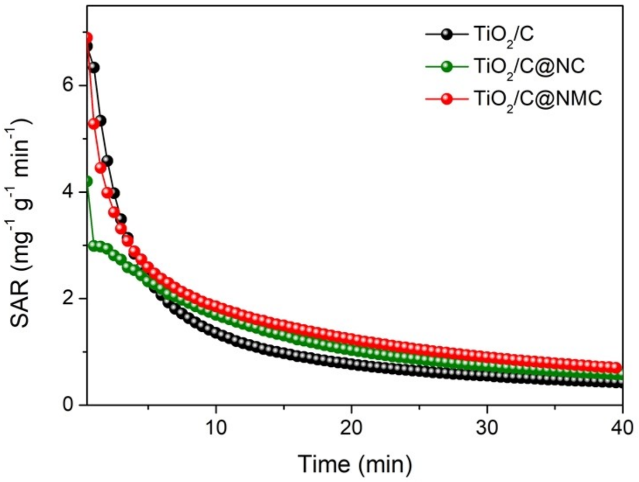

Fig. S15. The SAR variations versus time f TiO_2/C, TiO_2/C@NC, and TiO_2/C@NMC.

Table S3. The charge efficiency (Λ) and energy consumption (E) of TiO_2/C, TiO_2/C@NC, and TiO_2/C@NMC.

Sample	Charge efficiency (%)	Energy consumption (kWh kg_{NaCl}^{-1})
TiO_2/C	73.1	0.75
TiO_2/C@NC	79.4	0.69
TiO_2/C@NMC	87.3	0.61

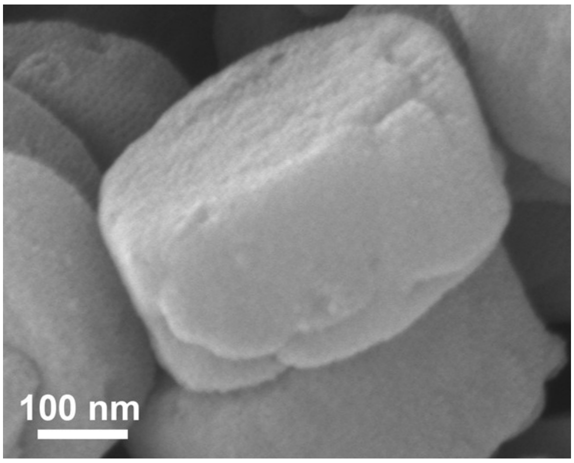

Fig. S16. SEM image of TiO_2/C@NMC after regeneration tests.

Table S4. Comparison of TiO_2/C@NMC and other reported electrode materials.

Electrode materials	**Voltage (V)**	**NaCl concentration (mg L^{-1})**	**SAC (mg g^{-1})**	**Ref.**
rGO/T2	1.2	300	16.4	1
rGO-15TiO_2	1.2	75	24.58	2
TiO_2@CNTs	1.4	25-800	4.0	3
TiO_2/carbon	1.2	280	17.4	4
MoS_2/graphene	1.2	500	19.4	5
MnO_x nanofiber	1.2	877	27.8	6
Open and interconnected porous architectures	1.2	500	14.35	7
Nitrogen-doped activated carbon	1.2	468	24.7	8
Sugarcane Biowaste-Derived Biochars	1.2	600	21.8	9
ZIF-8@PZS-C	1.2	500	22.19	10
TiO_2@COF-2	1.4	200	26.0	11
TiO_2/C@NMC	1.2	250	27.73	This work
TiO_2/C@NMC	1.6	250	35.54	This work

References

1 A. G. El-Deen, J.-H. Choi, C. S. Kim, K. A. Khalil, A. A. Almajid and N. A. M. Barakat, *Desalination*, 2015, **361**, 53-64.

2 H. M. Moustafa, M. Obaid, M. M. Nassar, M. A. Abdelkareem and M. S. Mahmoud, *Sep. Purif. Technol.*, 2020, **235**, 116178.

3 H. Li, Y. Ma and R. Niu, *Sep. Purif. Technol.*, 2016, **171**, 93-100.

4 P. Srimuk, M. Zeiger, N. Jäckel, A. Tolosa, B. Krüner, S. Fleischmann, I. Grobelsek, M. Aslan, B. Shvartsev, M. E. Suss, *Electrochim. Acta*, 2017, **224**, 314-328.

5 J. Han, T. Yan, J. Shen, L. Shi, J. Zhang, D. Zhang, *Environ. Sci. Technol.*, 2019, **53**, 12668-12676.

6 B. W. Byles, D. A. Cullen, K. L. More, E. Pomerantseva, *Nano Energy*, 2018, **44**, 476-488.

7 Y. Zhu, G. Zhang, C. Xu and L. Wang, *ACS Appl. Mater. Interfaces*, 2020, **12**, 29706-29716.

8 C. C. Hsu, Y. H. Tu, Y. H. Yang, J. A. Wang and C. C. Hu, *Desalination*, 2020, **481**, 114362.

9 J. J. Lado, R. L. Zornitta, I. V. Rodríguez, K. M. Barcelos and L. A. M. Ruotolo, *ACS Sustainable Chem. Eng.*, 2019, **7**, 18992-19004.

10 J. Zhang, J. Fang, J. Han, T. Yan, L. Shi and D. Zhang, *J. Mater. Chem. A*, 2018, **6**, 15245-15252.

11 X. Liu, S. Zhang, G. Feng, Z.-G. Wu, D. Wang, M. D. Albaqami, B. Zhong, Y. Chen, X. Guo, X. Xu, and Y. Yamauchi, *Chem. Mater.*, 2021, **33**, 1657-1666.